Gap-Townes solitons and localized excitations in low-dimensional Bose-Einstein condensates in optical lattices

Fatkhulla Kh. Abdullaev*

*Dipartimento di Fisica "E.R. Caianiello," Universitá di Salerno, I-84081 Baronissi (SA), Italy,
and Physical-Technical Institute of the Academy of Sciences, 700084, Tashkent-84, G.Mavlyanov str., 2-b, Uzbekistan*

Mario Salerno†

*Dipartimento di Fisica "E.R. Caianiello," Consorzio Nazionale Interuniversitario per le Scienze Fisiche della Materia (CNISM),
Istituto Nazionale di Fisica Nucleare (INFN), Sezione di Napoli-Gruppo Collegato di Salerno, Universitá di Salerno,
I-84081 Baronissi (SA), Italy*

We discuss localized ground states of Bose-Einstein condensates (BEC's) in optical lattices with attractive and repulsive three-body interactions in the framework of a quintic nonlinear Schrödinger equation which extends the Gross-Pitaevskii equation to the one-dimensional case. We use both a variational method and a self-consistent approach to show the existence of unstable localized excitations which are similar to Townes solitons of the cubic nonlinear Schrödinger equation in two dimensions. These solutions are shown to be located in the forbidden zones of the band structure, very close to the band edges, separating decaying states from stable localized ones (gap solitons) fully characterizing their delocalizing transition. In this context the usual gap solitons appear as a mechanism for arresting the collapse in low-dimensional BEC's in optical lattices with an attractive real three-body interaction. The influence of the imaginary part of the three-body interaction, leading to dissipative effects in gap solitons, and the effect of atoms feeding from the thermal cloud are also discussed. These results may be of interest for both BEC's in atomic chips and Tonks-Girardeau gas in optical lattices.

I. INTRODUCTION

Bose-Einstein condensates (BEC's) in periodic potentials are presently receiving a great deal of theoretical and experimental interest due to the possibility to explore a whole class of phenomena ranging from Bloch oscillations [1,2], Landau-Zener tunneling [3], and solitons [4] to quantum phase transitions of the Mott insulator type [5]. In the mean-field approximation these systems are described by the Gross-Pitaevskii equation (GPE) which is a cubic nonlinear Schrödinger (NLS) equation with periodic potential in which the cubic nonlinearity models the two-body interatomic interactions appropriate for dilute gases. The presence of the optical lattice (OL) allows interesting localization phenomena such as the formation of gap solitons—i.e., localized states with energies comprised in the gaps of the band structure of the underlying linear periodic problem—for both attractive and repulsive interactions [6,7]. This is quite remarkable because it is known that for two- (2D) and three- (3D) dimensional NLS equations, in the absence of a periodic potential, soliton solutions do not exist and for attractive interactions the phenomenon of collapse in finite time appears. In this last case only one localized solution is possible, the so-called Townes soliton, existing for a single value of the norm (number of atoms). This solution, however, is unstable against norm variations; i.e., it collapses in a finite time for

norms above the critical value and decays into the uniform background for norms below the critical value. The presence of the OL allows one to expand the range of the existence of localized solutions from a single value to a whole interval of norms below which the delocalizing transition occurs and above which collapse takes place.

A description based on the GPE with cubic nonlinearity, however, is adequate only at low densities. For higher densities three-body interactions start to play a role and a description based on two-body interactions is no longer sufficient [8–11]. In this regard we recall that condensate densities limited by three-body inelastic collisions [12] have indeed been achieved. In these regimes a more accurate treatment of the mean-field energetics of a dense condensate will need to account for both two- and three-body elastic collisions.

Contribution of the three-body interactions can be enhanced by detuning to zero the cubic two-body term by means of Feschbach resonances [12], this leading to a periodic NLS equation with quintic nonlinearity. For appropriate values of density and scattering lengths, however, the three-body collisions could largely dominate the two-particle contributions even in a very dilute regime. This occurs when the so-called Efimov effect [13] becomes possible and the two-body scattering length becomes much larger than the effective two-body interaction radius (this usually occurring near a two-body resonance). In this case a very large number of three-body bound states can be formed in the system and the contribution of the three-body elastic collisions (cubic in the density) to the energy may largely overcome the one arising

*Electronic address: fatkh@physic.uzsci.net
†Electronic address: salerno@sa.infn.it

from the two-body terms (quadratic in the density). In this situation the condensate appears extremely dilute with respect to the two-body collisions but somewhat dense with respect to the three-body collisions [14].

Theoretical estimates of the three-body coefficient were given in Refs. [15–18]. This term can be modeled by a quintic nonlinearity in the GPE which for rubidium atoms is expected to be attractive [9]. The different types of instabilities induced by the quintic term may lead to interesting dynamical phenomena in 1D BEC's similar to the Bose-Novae effect observed in the multidimensional case. On the other hand, the presence of these instabilities restricts the possibility of BEC manipulations in atomic waveguides [9,10]. The optical lattice, however, can suppress or delay some of these instabilities, opening the possibility for new types of localized excitations.

The 1D quintic NLS equation is also used to describe a Bose gas with hard-core interactions in the Tonks-Girardeau regime. Recent works have shown that this approach describes well the ground-state properties, the collective oscillations in a parabolic trap [20], and the dynamics of shock waves and dark solitons in the gas [21,22]. On the other hand, interference phenomena generated with a small number of atoms ($N=10$) were shown to be not well accounted for by the quintic NLS equation (the interference patterns obtained from this equation are much more pronounced than the experimental ones) [23]. For a larger number of atoms and for weak density modulations, however, the description of the nonlinear excitations in the Tonks-Girardeau regime by means of a quintic NLS equation is expected to be valid.

The aim of the present paper is to study localized states of the quintic nonlinear Schrödinger equation with a periodic potential for both attractive and repulsive interactions. In this regard we use a variational method, a self-consistent approach, and direct numerical integrations to show that the presence of the optical lattice allows us to stabilize solitons of the attractive quintic 1D NLS equation against collapse or decay. In the case of repulsive interactions the optical lattice is found to be crucial for the existence of stable bright matter waves. The existence of localized excitations in this system is shown to be associated with the existence of unstable localized solutions similar to the Townes soliton of the cubic 2D NLS equation (we refer to them as gap-Townes solitons). These unstable solutions are found to be located in the forbidden zones of the band structure, very close to band edges and separate decaying states from stable gap solitons. The existence curve of these solutions characterizes the critical threshold for the occurrence of the delocalizing transition, and the existence of gap solitons appears to be a mechanism for arresting collapse in 1D BECs in OLs with three-body interactions. We also investigate dissipative effects in gap solitons induced by the imaginary part of the three-body interactions. We show that when the imaginary part of this interaction is small compared to the real part, localized states exist for very long times and their behavior is qualitatively similar to the one of the undamped case. For moderate and large damping, however, all localized states in the band gap decay into the Bloch state at the band edge. We find it remarkable that even in this case a reminiscence of the existence of gap-Townes solitons survives in focusing-

defocusing cycles observed when the number of atoms is close to the critical value for their existence. We also find that these localized states can be stabilized into breatherlike excitations by a linear amplification term modeling the feeding of atoms in the condensate from the thermal cloud in the presence of nonlinear damping.

We remark that in the absence of a periodic potential the quintic 1D NLS equation has a behavior similar to the 2D NLS equation with cubic nonlinearity. The interplay between dimensionality and nonlinearity has indeed been used in the past to investigate the collapse in lower-dimensional NLS equations, the critical condition being $D(n-1)-4=0$ where n is the order of the nonlinearity in the equation and D is its dimensionality [24]. From this point of view the quintic NLS equation can be viewed as a 1D model for the 2D GPE with cubic mean-field nonlinearity and we expect that the results discussed in this paper will apply also to this case.

The paper is organized as follows. In Sec. II we introduce the 1D model and discuss the range of applicability to different physical situations. In Sec. III we study the quintic 1D NLS equation with attractive interactions in both the absence and presence of a periodic potential. The effectiveness of the optical lattice to stabilize localized states of the GPE in the presence of two-body and three-body interactions is investigated by means of a variational analysis and by direct numerical simulations. We use a self-consistent method to investigate gap solitons and band structures. The existence of gap-Townes solitons is shown in Sec. IV, and the role of the usual gap solitons in arresting collapse is discussed. In Sec. V we investigate the case of repulsive interactions by means of a variational analysis, self-consistent method, and numerical simulations. The existence of unstable Townes solitons with energies above the band edges and their role in the delocalizing transition is also investigated. In Sec. VI the dissipative effects introduced by an imaginary part of the three-body interaction on gap solitons are studied by both a modified variational analysis and direct numerical simulations. The effects of atoms feeding from the thermal cloud are also considered. Finally, in the last section, the main results of the paper are briefly discussed and summarized.

II. MODEL

Let us consider a BEC with two- and three-body interactions immersed in an optical lattice and a highly elongated harmonic trap. In the mean-field approximation the system is described by the 3D GPE [10]

$$i\hbar u_t = -\frac{\hbar^2}{2m}\nabla^2 u + \left[\frac{m}{2}(\omega_\perp^2 \rho^2 + \omega_x^2 x^2) + V_{opt}(x)\right]u$$
$$+ g_1|u|^2 u + g_2|u|^4 u, \tag{1}$$

with ρ denoting the radial distance, g_1 and g_2 the nonlinear coefficients corresponding to the two- and three-body interactions, respectively, $\omega_\perp$ and ω_x the radial and longitudinal frequencies of the anisotropic trap ($\omega_\perp \gg \omega_x$), and $V_{opt}(x) = V_0 \sin^2(kx)$ the optical lattice applied only in the longitudinal direction. The coupling constant of the two-body interaction is related to the s-wave scattering length a_s and to the

mass m of the atoms by the usual relation $g_1 = 4\pi\hbar^2 a_s/m$. In view of the strong anisotropy of the trap we can average the three-dimensional interaction over the radial density profile to reduce the problem to an effective one-dimensional one. More precisely, we consider solutions of the form $u(r,t) = \phi_0(\rho)\psi(x,t)$ where $\phi_0 = (\sqrt{1/\pi a_\perp^2})\exp(-\rho^2/2a_\perp^2)$ is the ground state of the radial linear equation

$$-\frac{\hbar^2}{2m}\nabla_\rho^2 \phi_0 + \frac{m}{2}\omega_\perp^2 \rho^2 \phi_0 = \hbar\omega_\perp \phi_0. \qquad (2)$$

Multiplying both sides of the GPE by ϕ_0 and integrating over the transverse variable, we obtain the quasi-1D GP equation [9]

$$i\hbar\psi_t = -\frac{\hbar^2}{2m}\psi_{xx} + \left(\frac{m}{2}\omega_x^2 x^2 + V_0 \sin^2(kx)\right)\psi$$

$$+ \frac{g_1}{2\pi a_\perp^2}|\psi|^2\psi + \frac{g_2}{3\pi^2 a_\perp^4}|\psi|^4\psi. \qquad (3)$$

For a discussion of the limits of applicability of this 1D reduction see Ref. [25]. Introducing the dimensionless variables

$$t = t\nu, \quad x = kx, \quad \nu = \frac{E_R}{\hbar}, \quad \alpha = \frac{\omega_x^2}{4\nu^2}, \qquad (4)$$

we reduce Eq. (3) to the following normalized 1D GPE with cubic and quintic nonlinearities:

$$i\psi_t = -\psi_{xx} + g|\psi|^2\psi + \chi|\psi|^4\psi + \alpha x^2\psi - \varepsilon\cos(2x)\psi, \quad (5)$$

where $a_s = a_{s0}g$, with a_{s0} the constant scattering length, $g \in [-1,1]$, and $E_R = \hbar^2 k^2/2m$ the recoil energy of the lattice. In this normalization the wave function has been scaled according to $\psi \rightarrow \psi\sqrt{2a_{s0}\omega_\perp/\nu}$ and the parameters ε and χ are defined as $\varepsilon = V_0/(2E_R)$ and $\chi = g_2(\nu/2a_{s0}\omega_\perp)^2/3\pi^2\hbar\nu a_\perp^4$. In the following we will be mainly interested in the case $g=0$ for which it is convenient to rescale the wave function as $\psi \rightarrow (g_2/3\pi^2 a_\perp^4 E_R)^{1/4}\psi$. In this case the relation between the dimensionless number of atoms, N, and the physical one, N_p, is $N_p = [3\pi^2 a_\perp^4 E_R/(g_2 k^2)]^{1/2}N$ (the values of N_p are typically in the range 4000–5000 for $g_2/\hbar \approx 10^{-26}$ cm^6 s^{-1}, $a_\perp = 2$ μm, $\lambda = 8.23 \times 10^{-7}$ m, and $m = 1.44 \times 10^{-25}$ kg).

Equation (5) is obtained from the Hamiltonian

$$H = \int_{-\infty}^{\infty} dx\left[|\psi_x|^2 + \frac{g}{2}|\psi|^4 + \frac{\chi}{3}|\psi|^6 + V(x)|\psi|^2\right], \qquad (6)$$

as $i\psi_t = \delta H/\delta\psi^*$. This equation appears also in the context of nonlinear photonic crystals [26]. The relevance of the two-body interactions (cubic term) for the formation of localized excitations of soliton type has been largely investigated in the past decades in the field of nonlinear optics, and the existence of bistable solitons in optical media with Kerr (cubic) and saturable (quintic) nonlinearity was established for the case of a channel waveguide with step potential [26].

The cubic-quintic NLS equation also appears as a model for the propagation of optical pulses in double-doped optical fibers [27] with an effective refraction index given by $n = n_2 + n_4|E|^2$, where $n_2 = n_{d_1} + n_{d_2}$, $n_4 = n_{d_2}$, and n_{d_i} are the con-

tributions of dopants to the refraction index (values and signs can be changed by proper choice of dopants). Although Townes solitons have been presently found only in connection with collapse of 2D elliptic-shaped intensive beams in homogeneous focusing Kerr media [28], we expect gap-Townes solitons to be observed also in double-doped fibers with Bragg gratings, in the form of optical pulses, and in photonic crystal fibers, in the form of spatial optical solitons.

Finally, we remark that a pure quintic NLS equation with repulsive interactions also appears in connection with a Tonks-Girardeau gas in the local density approximation [19]. In this context the field equation is

$$i\hbar\phi_t = -\frac{\hbar^2}{2m}\phi_{xx} + V(x)\phi + \frac{\pi^2\hbar^2}{2m}|\phi|^4\phi, \qquad (7)$$

also written in normalized form as

$$iu_t + u_{xx} - \alpha x^2 u + \epsilon\cos(2x)u - |u|^4 u = 0, \qquad (8)$$

which corresponds to the case $g=0, \chi=1$ in Eq. (5). Here normalization has been made by introducing dimensionless variables $x = kx$, $t = t\nu$, $u = \phi\sqrt{\pi/k}$, with $\int dx|\phi|^2 = N_p = N/\pi$. In the next sections we use the variational approach [29], the self-consistent method [30], and direct numerical integrations to study localized states of the quintic NLS in presence of an optical lattice for both attractive and repulsive interactions.

III. ATTRACTIVE INTERACTIONS

To obtain analytical predictions for the existence of stable localized solutions of Eq. (5) with $\alpha=0$ and for attractive interactions [$g,\chi < 0$ in Eq. (5)], we use the variational approximation (VA) with a Gaussian ansatz for the fundamental soliton:

$$\psi(x,t) = A\exp\left(-i\mu t - \frac{1}{2}ax^2\right), \qquad (9)$$

with μ denoting the chemical potential and A and a amplitude and square root of the reciprocal width of the soliton, respectively. Following the standard VA (see Ref. [29] for a review) we derive the effective Lagrangian

$$\bar{L} = \frac{A^2\sqrt{\pi}}{2\sqrt{a}}\left(\mu - \frac{a}{2} + \varepsilon e^{-1/a} - \frac{gA^2}{2\sqrt{2}} - \frac{\chi A^4}{3\sqrt{3}}\right), \qquad (10)$$

from which the stationary equations $\partial\bar{L}/\partial a = \partial\bar{L}/\partial A = 0$ for parameters a and A are obtained as

$$\mu = -\frac{a}{2}\left(1 - \frac{2N^2\chi}{3^{3/2}\pi}\right) + \varepsilon\left(\frac{2}{a} - 1\right)e^{-1/a} + \frac{gN\sqrt{a}}{2\sqrt{2\pi}}, \qquad$$

$$\frac{2N^2\chi}{3^{3/2}\pi} + \frac{gN}{2\sqrt{2\pi a}} = \frac{2\varepsilon}{a^2}e^{-1/a} - 1. \qquad (11)$$

Here the number of atoms has been expressed in terms of a, A, as $N = A^2\sqrt{\pi/a}$. Note that for $\varepsilon=0$, $g=0$, Eqs. (11) predict a maximum value of N for the existence of solitons given by $N_{cr} = \sqrt{3^{3/2}\pi/(2\chi)}$. This value should be compared
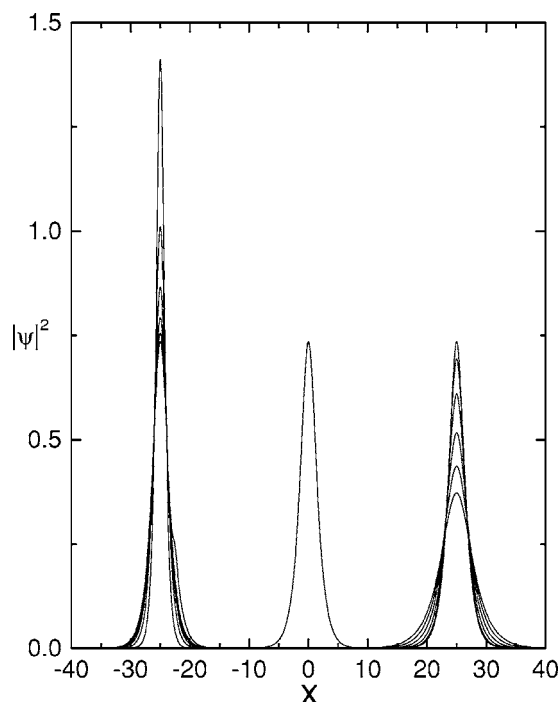
FIG. 1. Early stages of the evolution toward collapse (left curves) or decay (right curves) of the critical soliton (central curve) in the absence of external potentials ($\alpha=0$, $\varepsilon=0$). The critical soliton in the center refers to the value $\chi=-1$ and $N=2.7207$, while the collapse and decay evolution refer to $\chi=-1.01$ and $\chi=-0.99$, respectively, with all other parameters unchanged. Snapshots were taken at regular time intervals of 5.2 for collapse and of 10 for decay. Plotted quantities are in normalized units.

with the critical norm $N_{cr}^{(e)}=(\pi/2)\sqrt{3/|\chi|}$ obtained for the exact Townes soliton of Eq. (5) with $\varepsilon=0$, $g=0$, $\alpha=0$ [31]:

$$\psi_s = \exp(i\mu t)\psi, \quad \psi = \frac{(3\mu/|\chi|)^{1/4}}{\sqrt{\cosh(2\sqrt{\mu}x)}}. \quad (12)$$

We see that the VA value deviates from the exact one by only 5%. Notice that the above solution has zero energy and is marginally stable ($dN/d\mu=0$), so it exists only for the single value of the norm $N=N_{cr}^{(e)}$. Since for $N>N_{cr}^{(e)}$ the solution collapses in a finite time, while for $N<N_{cr}^{(e)}$ it decays into the uniform background, it appears as the analog of the Townes soliton of the cubic 2D NLS equation with attractive interactions. In Fig. 1 we depict the early stages of the time evolution toward collapse (decay) for an initial norm which is slightly increased (decreased) with respect to $N_{cr}^{(e)}$.

For $\varepsilon \neq 0$, Eq. (11) shows that the number of particles attains a minimum value $N_{thr}=[6\pi\sqrt{3}(1-8\varepsilon e^{-2})]^{1/2}$ at $a=1/2$; i.e., there exists a threshold value of the norm which is necessary to create a soliton. The expression for N_{thr} shows that the threshold exists for a relatively weak lattice and disappears if ε exceeds the value $\varepsilon_0=e^2/8\approx 0.9236$. From this analysis it is clear that the optical lattice is quite effective to stabilize solitons against decay when N is in the interval $N_{thr}<N<N_{cr}$. Collapse and decaying into extended states is

expected for $N>N_{cr}$ and $N<N_{thr}$, respectively. The VA makes it possible to predict the stability of the solitons on the basis of the *Vakhitov-Kolokolov* (VK) criterion [24], according to which a necessary condition for stability is given by $d\mu/dN<0$. Notice that the above variational equations are very similar to the ones derived in Ref. [32] for the 2D cubic NLS equation (with exactly the same value of ε_0), this being a further confirmation of the analogy between the 1D quintic NLS equation and the usual 2D GPE. We remark that, since N_{cr} does not depend on ε, the prediction of the VA is that the optical lattice does not affect collapse. We shall check these results in the next section.

IV. GAP-TOWNES SOLITONS AND ARRESTING COLLAPSE IN 1D BECs IN OLs

The existence of the exact Townes soliton (12) of the quintic NLS equation with $\varepsilon=0$ makes it natural to ask whether this solution could exist also in presence of the OL. In view of the analogies between the 1D quintic NLS equation and 2D GPE, the existence of this solution for $\varepsilon \neq 0$ could shine some light on the role of the OL in controlling collapse, as well as on the origin of the delocalizing transition observed in these systems [33]. In the following we use a self-consistent approach [30] to determine the critical value of N for the unstable solution to exist.

In Fig. 2(a) we report the band structure and localized states obtained with the self-consistent approach for the case $g=0$, $\alpha=0$ in Eq. (5). We see that there are two bound-state levels just below the band. The level closer to the band edge (open circle) corresponds to an unstable localized state while the other corresponds to a stable gap soliton. The corresponding wave functions are depicted in Figs. 2(b) and 2(c), respectively. We find that for a fixed value of ε there is only one value N for which the unstable state exists and its behavior resembles the one of the Townes soliton depicted in Fig. 1. In this case, however, we have that for a slightly overcritical value of N the unstable soliton starts to shrink and its energy decreases as for collapsing solutions until it reaches the gap soliton level below, at which the shrinking stops. The transition from the unstable Townes soliton to the stable gap soliton is represented in Fig. 2(a) by the lower arrow. If the norm is slightly decreased below N_{cr}, the unstable state completely delocalizes into the Bloch state at the bottom of the band shown in Fig. 2(d) [this decay is represented in Fig. 2(a) by the upper arrow]. Due to this behavior, we refer to the unstable state as a *gap-Townes soliton*, this name being also justified by the fact that for $\varepsilon \rightarrow 0$ the critical norm reduces to N_{cr}^e (see the left panel of Fig. 4). The decaying property of the gap-Townes soliton is illustrated in Fig. 3 where the time evolution obtained from direct numerical integrations of Eq. (5) (with $g=0$, $\alpha=0$) is shown. The left (right) panel of this figure shows the decay into the extended state (gap soliton) when the initial norm is slightly decreased (increased) with respect to N_{cr}. Notice that the transition into the gap soliton state is much more rapid than the decay into the extended state, this being a reminiscence of the collapse occurring at $\varepsilon=0$. Since the energy of a slightly overcritical gap-Townes solution should go to $-\infty$, as for any collapsing
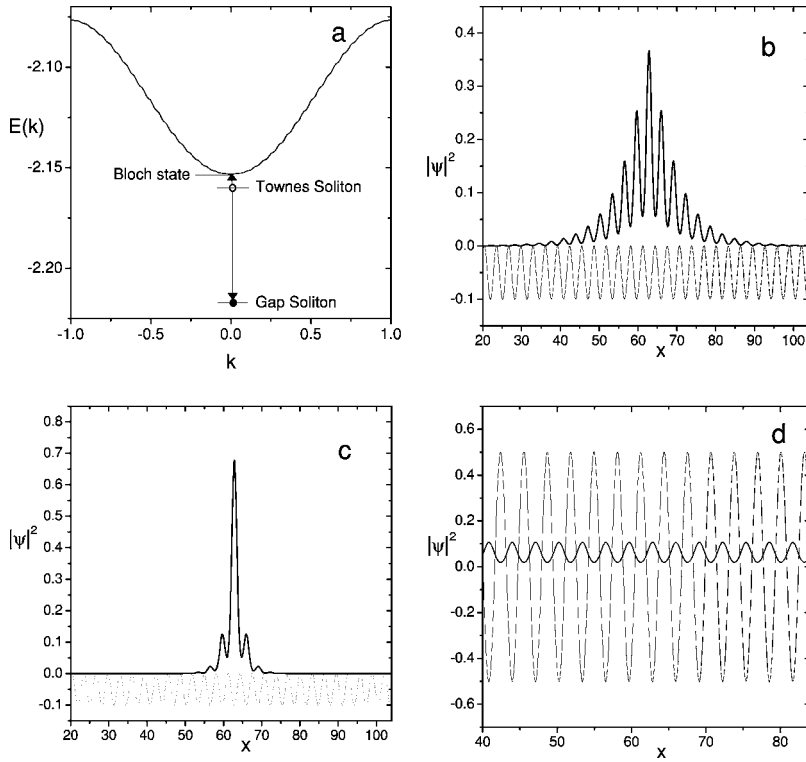
FIG. 2. (a) Lower band and localized bound states of the quintic NLS equation with attractive interactions for parameter values $\chi=-1$, $\varepsilon=5$. The arrows show the decay pattern of the gap-Townes bound state (open circle) for $N<N_{cr}$ (upper arrow) and $N>N_{cr}$ (lower arrow). (b) Gap-Townes soliton (thick line) corresponding to the unstable bound state level (open circle) in panel (a), with $N=N_{cr}=0.4616$ and $E=-2.1576$. (c) Gap soliton [thick line and solid circle in panel (a)] obtained from the unstable gap-Townes state for a slightly above critical value of N ($N=0.4657$, $E=-2.2177$). (d) The Bloch state (thick line) at the bottom of the band into which the gap-Townes soliton decays for a slightly subcritical value of N ($N=0.4586$, $E=-2.1531$). The OL is depicted as a thin dotted line scaled by a factor of 100 and shifted down by 0.05 in panels (b), (c) and scaled by a factor of 10 in panel (d). Plotted quantities are in normalized units.

solution, we see that the existence of a stable localized state which lies in energy below the unstable state is indeed a mechanism for arresting collapse in the system. Also note that a gap-Townes soliton appears as a separatrix between localized and extended states. The fact that its energy lies below the lower band edge implies the existence of a delocalizing threshold in the number of atoms below which localized state of the quintic GPE with OL cannot exist, this being a remarkable difference between cubic and quintic nonlinearities (in the cubic case the threshold exists only in the higher-dimensional case [33]). In Fig. 4(a) the threshold curve separating localized and extended states in the (N,ε) plane is depicted (this curve coincides with the norm of the gap-Townes soliton as a function of ε). Notice that for ε

$=0$ the norm coincides with the exact value $N_{cr}^{(e)}$ of the solution in Eq. (12), suggesting that the family of gap-Townes soliton for $\varepsilon \neq 0$ originates from the Townes soliton state at $\varepsilon=0$.

Numerical investigations show that collapse occurs when the strength of the optical lattice becomes small and the number of atoms overcomes the critical threshold for the Townes soliton at $\varepsilon=0$. For larger values of N the width of the soliton becomes small compared to the period of the periodic potential and the OL becomes ineffective for arresting collapse. We find that solitons extended on several potential wells are the ones which are better stabilized by the optical lattice against collapse. An indication of the occurrence of collapse at small values of ε is obtained from the
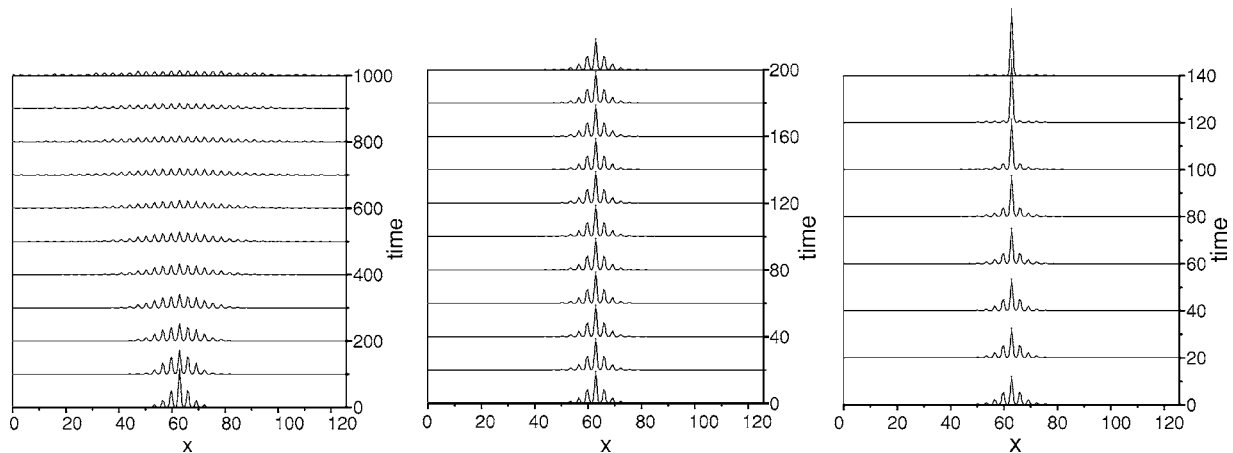

FIG. 3. Time evolution of the gap-Townes soliton in Fig. 2 (central panel) compared with the one obtained from numerical integration of the quintic NLS equation with two slightly different values of N: $N=1.1N_{cr}$ (right panel) and $N=0.9N_{cr}$ (left panel). Parameters are fixed as in Fig. 2, and plotted quantities are in normalized units.
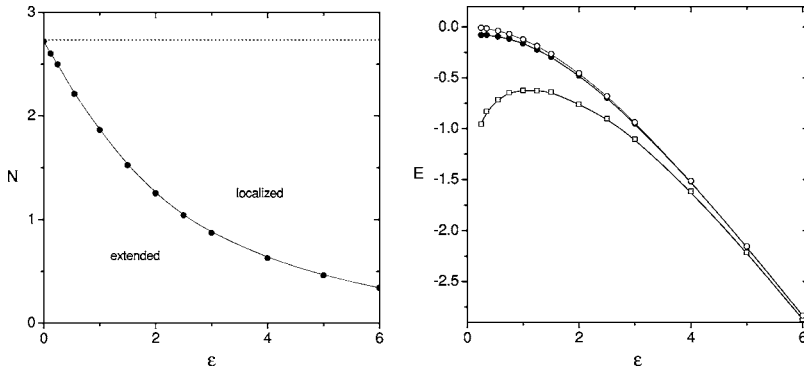
FIG. 4. Left panel: delocalizing transition threshold obtained by direct numerical integrations (solid circles) of the quintic [$g=\alpha=0$ in Eq. (5)] NLS equation with $\chi=-1.0$. The horizontal dotted line corresponds to the critical threshold for collapse in absence of the OL: $N_{cr} = (\pi/2)\sqrt{3/\chi}$. Right panel: energies versus ε of the gap soliton (bottom curve with open squares), gap-Townes soliton (middle curve with solid circles), and Bloch state at the bottom of the band (top curve with open circles) for the quintic NLS equation with $\chi=-1.0$. Plotted quantities are in normalized unit.

right panel of Fig. 4, in which we depict the energies of the Bloch state at the bottom of the band, of the gap-Townes soliton immediately below the band, and of the gap soliton, reported as a function of ε. We see that while the energies of the Bloch state and of the gap-Townes soliton monotonically increase with decreasing ε; the energy of the gap soliton reaches a maximum around $\varepsilon \approx 1$ and then starts to decrease as $\varepsilon \to 0$. This behavior is consistent with the fact that a collapsing solution with energy equal to $-\infty$ should exist at $\varepsilon=0$. A study of collapse for small ε, however, is numerically difficult to perform and requires more investigations. It is interesting to note that besides stable gap soliton the OL allows the existence of metastable states which are symmetric around a maximum of the potential (instead of a minimum as for the usual gap solitons). These intersite symmetric states have higher energy than the on-site symmetric ones and decay into the ground state after some time. Such states can be used to delay the time of collapse for $N > N_{cr}$. Indeed, the collapse of these metastable states begins when their instability sets in, as one can see from Fig. 5 (notice that the matter moves first into a single potential well and then starts to collapse).

V. REPULSIVE INTERACTIONS

To investigate the existence of localized states in the repulsive quintic NLS equation with periodic potential we apply first a variational analysis based on the following ansatz for the soliton wave form [33]:

$$\psi(x,t) = A \frac{\sin(ax)}{ax} \exp(-i\mu t). \quad (13)$$

Performing the same analysis as before, we get the averaged Lagrangian

$$\bar{L} = \frac{A^2 \pi}{2a} \left[\mu - \frac{a^2}{3} + \varepsilon\left(1 - \frac{1}{a}\right) - \frac{11\chi A^4}{60} - \frac{gA^2}{3} \right], \quad (14)$$

from which the following equations for the soliton parameters are obtained:

$$\mu = \varepsilon\left(\frac{2}{a} - 1\right) - \frac{1}{3}a^2 + \frac{11\chi N^2 a^2}{60\pi^2} + \frac{gNa}{3\pi},$$

$$\frac{N^2\chi}{\pi^2} + \frac{10gN}{11\pi a} = \frac{20}{11}\left(\frac{3}{2}\frac{\varepsilon}{a^3} - 1\right). \quad (15)$$

Using the fact that norm and soliton parameters are related by $N = \pi A^2 / a$, one can show that

$$A = \left[\frac{30N^3\varepsilon}{2\pi(11N^2|\chi| + 20\pi^2)} \right]^{1/6}; \quad (16)$$

i.e., the VA predicts the existence of a single set of soliton parameters a, A for a given norm N and strength ε of the OL. This is similar to what obtained in Ref. [33] for the localized solutions of the repulsive 2D GPE with OL. In the case of a Tonks-Girardeau gas in the OL these parameters can be estimated as follows. From Eq. (16) we get that $A \approx (30N\varepsilon/22\pi)^{1/6}$, and from the expression of N we get for the soliton width $w = 1/a \approx [22N^2/(30\pi^2\varepsilon)]^{1/3}$. For a number
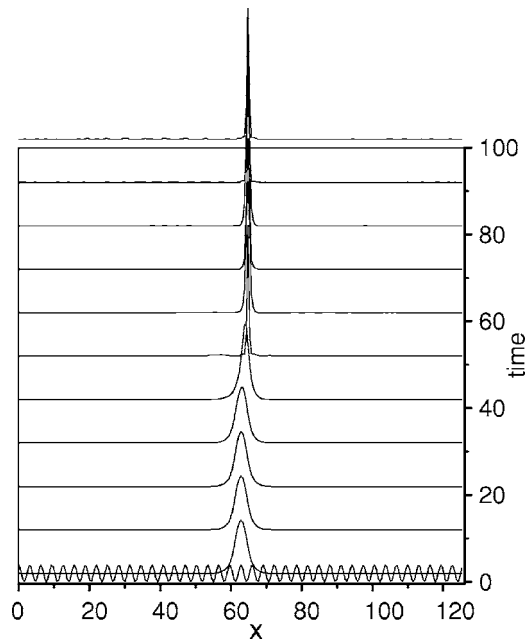

FIG. 5. Time evolution of an intersite symmetric intrinsic localized mode for the quintic NLS with $\chi=-1$, $N=2.847$ and $\epsilon=0.1$. Notice that collapse starts after the mode has decayed into an on-site symmetric one (ground state). The periodic potential is shown together with the initial state at $t=0$. Plotted quantities are in normalized units.
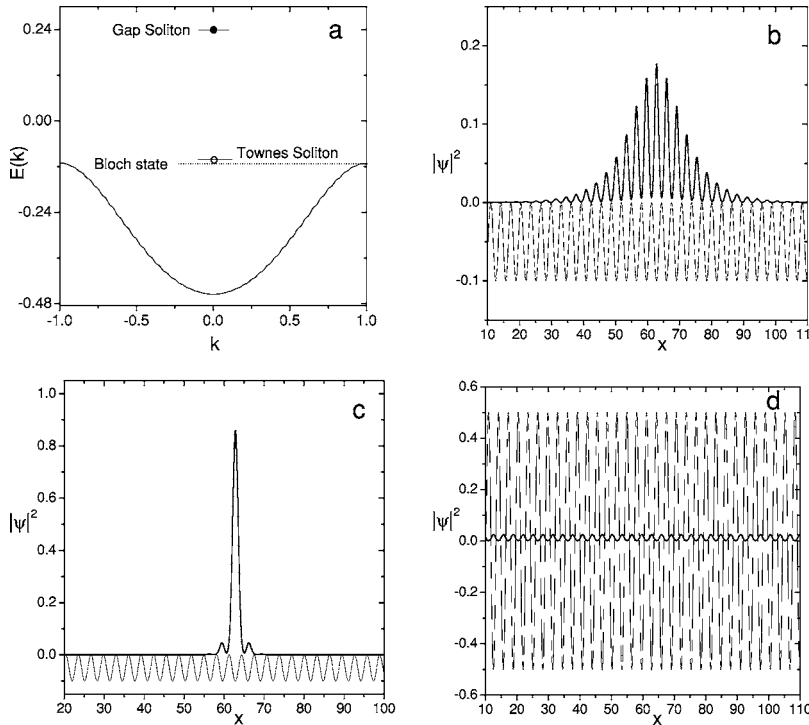
FIG. 6. (a) Lower band and localized bound states of the quintic $[g=\alpha=0$ in Eq. (5)$]$ NLS equation with repulsive interactions for parameter values $\chi=1$, $\varepsilon=2.0$. The arrows show the decay pattern of the gap-Townes bound state (open circle) for $N<N_{cr}$ (upper arrow) and $N>N_{cr}$ (lower arrow). (b) Gap-Townes soliton (thick line) corresponding to the unstable bound state level (open circle) in panel (a), with $N=N_{cr}=1.5565$ and $E=-0.1047$. (c) Gap soliton [thick line and solid circle in panel (a)] obtained from the unstable gap-Townes state for a slightly above critical value of N ($N=1.5965$, $E=0.2537$). (d) The Bloch state (thick line) at the bottom of the band into which the gap-Townes soliton decays for a slightly subcritical value of N ($N=1.5065$, $E=-0.1097$). The OL is depicted as a thin dotted line scaled by a factor of 20 and shifted down by 0.05 in panels (b),(c) and scaled by a factor of 10 in panel (d). Plotted quantities are in normalized units.

of particles $N=314$ (corresponding in physical units to $N_p=100$) and for $V_0=4E_R$, so $\varepsilon=2$, the width of the gap soliton is estimated to be $w\approx 15.5$, corresponding to three to four lattice periods.

The band structure associated with gap solitons of the repulsive quintic NLS equation has been investigated by means of the self-consistent method. In Fig. 6(a) we show the lower band and localized bound states for the case $g=0$, $\alpha=0$ in Eq. (5). We see that above the band edge there are two bound-state levels, one immediately above (open circle) corresponding to an unstable gap-Townes soliton, the other more separated from the band edge corresponding to a gap soliton. The wave functions of these bound states are depicted in Figs. 6(b) and 6(c). In analogy with the attractive

case, we have that the unstable soliton exists only for a critical value N_{cr} of the norm and has a behavior similar to the gap-Townes soliton described before. The decaying property of the repulsive gap-Townes soliton is clearly illustrated in Fig. 7 where we show the time evolution, as obtained from direct numerical integrations of Eq. (5) (with $g=0$, $\alpha=0$), of the gap-Townes soliton in Fig. 6(b) (central panel). The left and right panels of this figure show the decays into the extended (Bloch) and localized (gap soliton) states when the norm of the initial condition is, respectively, slightly decreased or increased with respect to N_{cr}. Thus, also in this case a gap-Townes soliton appears as a separatrix between localized and extended states. We remark, however, that in this case the existence of gap solitons is a direct consequence
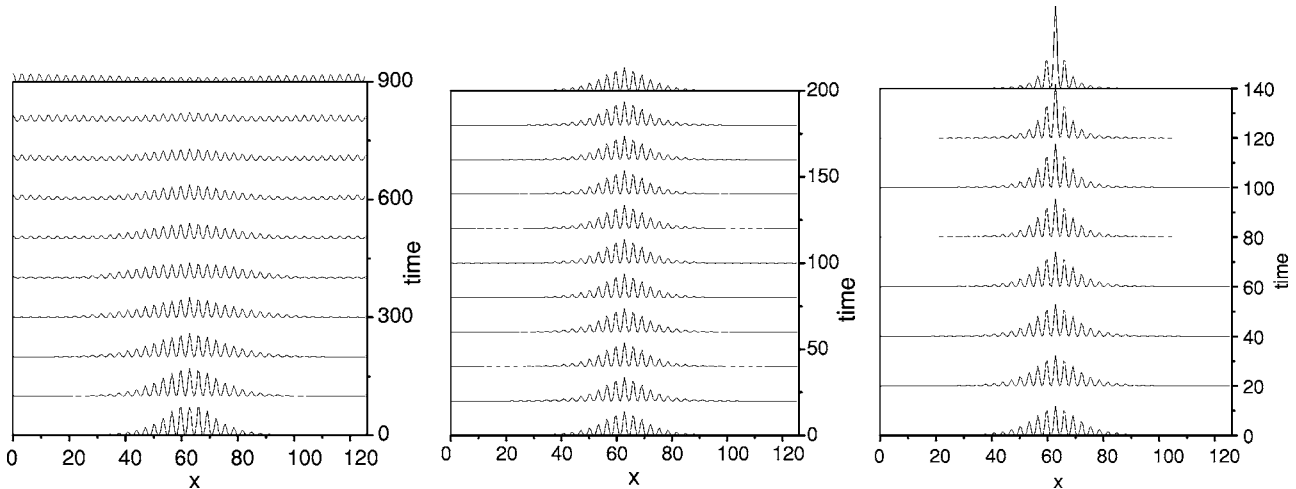

FIG. 7. Time evolution of the gap-Townes soliton in Fig. 6 as obtained from numerical integration of the quintic NLS equation with repulsive interaction and three slightly different values of number of atoms: $N_{cr}=1.5565$ (central panel), $N=1.05N_{cr}$ (right panel), and $N=0.95N_{cr}$ (left panel). Other parameters are fixed as in Fig. 6. Plotted quantities are in normalized units.
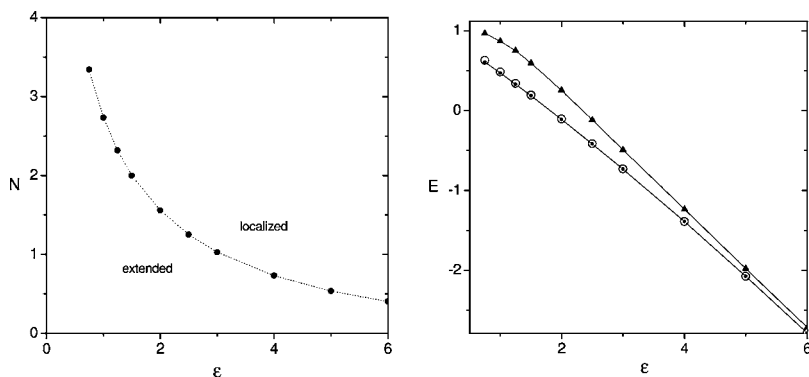
FIG. 8. Left panel: delocalizing transition threshold obtained by direct numerical integrations (solid circles) of the quintic NLS equation with $\chi = 1.0$. Right panel: energies versus ε of the gap soliton (top curve with solid triangles), gap-Townes soliton (curve with solid circles), and Bloch state at the top of the band (curve with open circles) for the quintic NLS equation with $\chi = 1.0$. Plotted quantities are in normalized units.

of the band structure (it could not exist without the OL). The fact that the energy of the Townes soliton is slightly above the upper band edge is consistent with the existence of a threshold in the number of atoms (given by the critical norm of the gap-Townes soliton) below which localized state of the quintic GPE with OL cannot exist. In the left panel of Fig. 8 we show the delocalizing curve in the plane (N, ε) separating localized from extended states. This behavior is very similar to what was reported for repulsive 2D solitons of the GPE in optical lattices [33]. In the right panel of the same figure we show the energies of the Bloch states at the top of the band, of the Townes soliton immediately above the band, and of the gap soliton, as a function of ε. In contrast with the attractive case we see that all energies monotonically increase with decreasing ε. The absence of a maximum in the energy curve of the gap soliton at small values of ε also indicates the absence of collapse in this case (compare the right panels of Figs. 4 and 8).

VI. GAP-TOWNES SOLITONS IN THE PRESENCE OF DISSIPATION

In the previous sections we have investigated the general properties of localized states of 1D BECs in OLs with the elastic three-body interactions modeled by a real quintic nonlinearity. It is known, however, that the three-body interaction bears also an imaginary component corresponding to inelastic collisions which can be modeled by a damping term of the form $-i\gamma|\psi|^4\psi$ on the right-hand side of Eq. (5). Recent theoretical studies [15–18] estimate for Rb a negative value of the real part of the quintic nonlinearity of the order of 10^{-26}–10^{-27} cm^6/s. From the experiment in Ref. [34] one can deduce the imaginary part of the three-body interaction for Rb to be of the order 10^{-30} cm^6/s. These numbers imply a ratio between the imaginary and real parts of this interaction of the order of 10^{-3}–10^{-4}. Other data give values of the damping constant of the order of 10^{-28} cm^6/s. Due to the uncertainty intrinsic in some of these numbers (presently there are no measurements of the real part of the three-body interactions), in the following we take the damping constant γ to be a free parameter and investigate both the underdamped and overdamped regimes.

The instability of gap-Townes solitons against small fluctuations in the number of the atoms raises the question of how the scenario of the previous sections changes in presence of dissipation. To answer this question we concentrate on the case of attractive quintic interactions (qualitatively similar results hold also for repulsive interactions) in the presence of a quintic dissipation. The results are displayed in Fig. 9. In the top three panels of this figure we depict the time evolution of the gap-Townes soliton in Fig. 2 in the presence of a small damping. We see that in spite of a slow broadening of the Townes soliton (middle panel), the situation remains qualitatively similar to the undamped case depicted in Fig. 3. Notice that for an overcritical number of atoms (right top panel) several focusing-defocusing cycles between the gap-Townes soliton and the gap soliton occur (these oscillations are induced by the slightly overcritical starting value of N). From the left panel of this figure we also see that for an undercritical number of atoms the decay into the Bloch states occurs faster than for the zero-damping case. At very long times the gap-Townes soliton in the middle panel of Fig. 9 eventually decays into the Bloch state at the edge of the band.

For larger damping the situation is different, as one can see from the bottom three panels of Fig. 9. Notice that for an overcritical value of N the gap-Townes soliton (right panel) decays into an extended state after performing only one focusing-defocusing cycle. In this case the dissipation completely suppresses collapse and localized states become unstable against decay into the lowest-energy Bloch state. It is remarkable, however, that a signature of the existence of gap-Townes solitons remains even for moderately large dampings in the focusing-defocusing cycles observed when the decreasing (due to dissipation) number of atoms crosses the critical value for the existence of gap-Townes solitons. This fact could indeed be used in experiments to detect the existence of gap-Townes solitons in the presence of damping.

An analytical explanation of the existence of focusing-defocusing cycles can be obtained by means of a modified variational analysis [35,36] in which the damping is treated as a small perturbation. In this approach we assume a time-dependent localized state of the form

$$\psi(x,t) = A \exp\left(-\frac{x^2}{2w^2} + ibx^2 + i\phi\right), \qquad (17)$$

with parameters $\eta_i \equiv \{A, w, b, \phi\}$ also time dependent. The equations of motion for these variables are obtained from the averaged unperturbed Lagrangian of Eq. (5) with $g=0$,
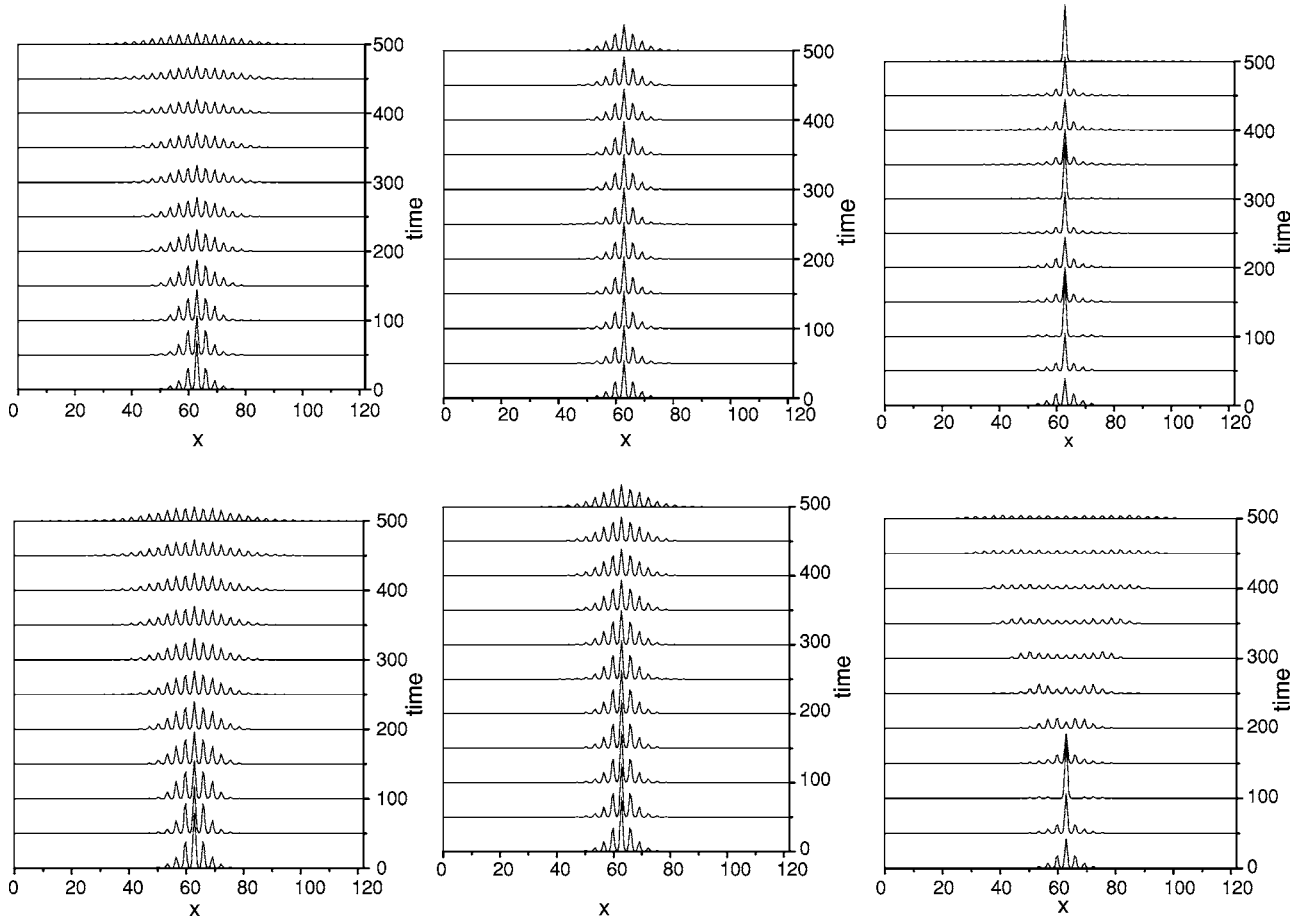
FIG. 9. Time evolution of gap-Townes soliton in Fig. 2 as obtained from numerical integration of the dissipative quintic NLS equation with attractive interaction. The top three panels refer to three slightly different values of number of atoms: $N_{cr}=0.87248$ (central panel), $N=1.1N_{cr}$ (right panel), and $N=0.9N_{cr}$ (left panel) with a dissipation parameter $\gamma=0.00025$. The bottom three panels are the same but for $\gamma=0.01$. Other parameters are fixed as $\chi=-1$, $\varepsilon=5$. Plotted quantities are in normalized units.

$$L = -\frac{\sqrt{\pi}}{2} A^2 w \left[w^2 b_t + 2\phi_t + \frac{1}{w^2} + 4w^2 b^2 - 2\varepsilon e^{-w^2} + \frac{2\chi}{3\sqrt{3}} A^4 \right],$$

as

$$\frac{d}{dt}\frac{\partial L}{\partial \eta_{i,t}} - \frac{\partial L}{\partial \eta_i} = \int_{-\infty}^{\infty} dx (R\psi_{\eta_i}^* + R^*\psi_{\eta_i}), \qquad (18)$$

where $R=-i\gamma|\psi|^4\psi$ and the subscript η_i denotes the derivative with respect to soliton parameters. From the above generalized Euler-Lagrange equation one derives the following equations for the number of atoms N and soliton width w:

$$N_t = -3\gamma\beta\frac{N^3}{w^2},$$

$$w_{tt} = \frac{4}{w^3}(1 + \chi\beta N^2) - 8\varepsilon we^{-w^2}, \qquad (19)$$

with $\beta=2/(3\sqrt{3}\pi)$.

In Fig. 10 we show the time evolution of the soliton width for different values of the dissipation constant. We see that for very low dampings the width oscillates around a constant value, meaning that the localized state undergoes periodic

focusing-defocusing cycles in agreement with the right top panel of Fig. 9. By increasing the damping we see that after a certain number of cycles, the soliton width starts to grow monotonically, signaling the decay of the gap soliton into an extended state. Notice that even for relatively high dampings there is one focusing-defocusing cycle, this being in good qualitative agreement with what is observed in the bottom right panel of Fig. 9. In the right panel of Fig. 10 we make a quantitative comparison between the dynamics of the soliton width as obtained from the VA and from the damped quintic NLS equation. From this figure we see that although the main feature of the phenomenon is correctly captured (i.e., the existence of only one focusing-defocusing cycle before decay), the variational equations are not in good quantitative agreement with numerical integration of the full system. This may be due to the fact that the ansatz in Eq. (17) is more appropriate for strongly localized states than for extended gap-Townes ones. It is interesting, however, that for $\epsilon=0$ the variational equations become similar in form to the ones considered for the 2D cubic NLS equation in the presence of a cubic dissipation $-i\gamma|\psi|^2\psi$ [37]. In this case one can show that the equation for w reduces to a modified Airy equation for which a focusing-defocusing cycle always exists. When $\epsilon \neq 0$, Eqs. (19) predict that for decreasing γ the number of
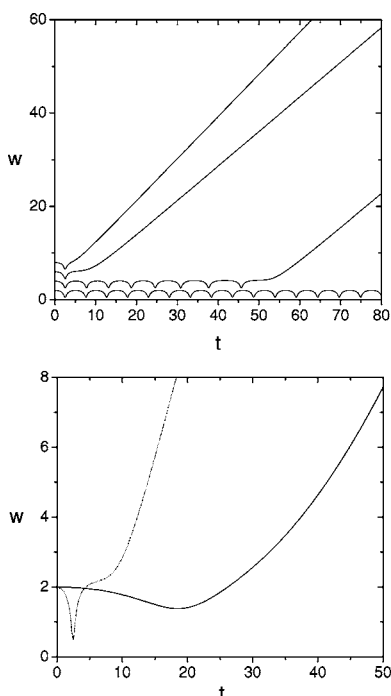
FIG. 10. Top panel: time evolution of the width of the gap-Townes soliton as obtained from Eqs. (19) with $\varepsilon=2$, $\chi=-1$, and damping parameters increased by a factor of 10 going from the bottom curve ($\gamma=0.0001$) to the top one ($\gamma=0.1$). The last three curves have been shifted, respectively, by 2, 4, 6, to avoid overlapping. The initial value of atoms was detuned from the critical value $N=1.254$ corresponding to the unperturbed gap-Townes by 0.05. Bottom panel: time evolution of the soliton width obtained from the damped quintic GPE (solid line) and from the variational equations (19) (dotted line). Parameter values are taken as $\varepsilon=2$, $\chi=-1$, and $\gamma=0.01$. Comparison with the variational results was done by rescaling the soliton width obtained from the GPE by a factor of 11.5 to have the same initial condition. Plotted quantities are in normalized units.

focusing-defocusing cycles grows, this being in good agreement with direct numerical simulations. Moreover, from the left panels of Figs. 4 and 8 we see that the critical value of the number of atoms for the existence of a gap-Townes soliton decreases by increasing ε, this meaning that in strong optical lattices the effect of the quintic damping on gap-Townes solitons is effectively reduced (due to the reduced

norm), this being confirmed also by numerical simulations.

We remark that besides the decay phenomena induced by the quintic dissipation one could also consider the feeding of atoms in the condensate from the thermal cloud [38]. The injection of matter in the BEC can be modeled with a linear imaginary term (of sign opposite to γ) in the NLS equation of the form $i\delta\psi$. This term can balance the damping and stabilize localized states against decay even in the over-damped regime, this leading to the formation of dissipative gap solitons. We illustrate this phenomenon in Fig. 11 where the time evolution of the slightly overcritical gap-Town soliton shown in the bottom right panel of Fig. 9 is reported for a linear amplification term of strength $\delta=8.95\times10^{-4}$. From this figure we see that the localized state, instead of decaying into the Bloch state at the bottom of the band (see Fig. 9), executes breatherlike oscillations (i.e., focusing-defocusing cycles) with the emission of radiation. In terms of the band picture this breathing state can be thought as a nonstationary state with energy oscillating between the gap-Townes soliton and the gap soliton in Fig. 2(a). We believe this is a general mechanism for the existence of breatherlike excitations in 1D BECs in OLs in the presence of damping and amplification.

VII. CONCLUSIONS

In this paper we have used the periodic 1D NLS equation with quintic nonlinearity to investigate localized states in 1D BECs in OLs with three-body interactions. The existence of unstable solitons similar to the usual Townes soliton of the cubic 2D NLS equation has been established. These states have been shown to have energy located in the forbidden zones of the band structure, very close to band edges, separating decaying states from stable localized ones (gap solitons). The existence of gap solitons appears to be a mechanism for arresting collapse in attractive low-dimensional BECs with three-body interactions in OLs, and the analysis of gap-Townes solitons appears to be important for characterizing the delocalizing transition in these systems. In this regard we remark that the region of the existence of localized states in the N, ε plane is bounded by two limiting curves. The first curve separates extended states from localized ones and therefore characterizes the delocalizing transition. This curve coincides with the curve of the existence of gap-
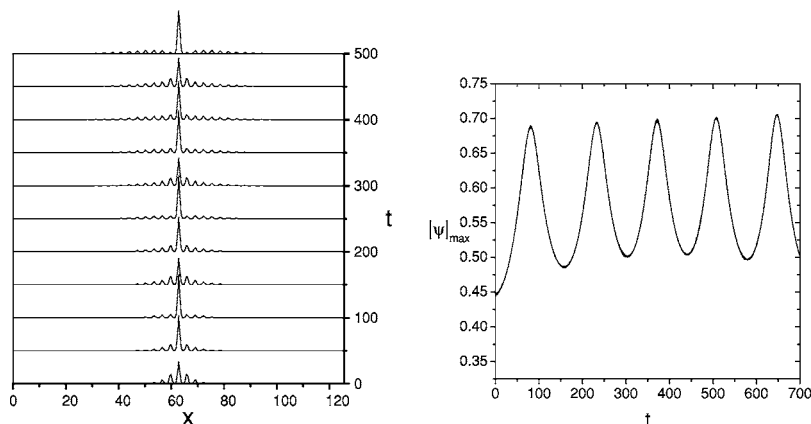

FIG. 11. Left panel: time evolution of the gap-Townes soliton in the lower right panel of Fig. 9 in the presence of quintic dissipation $\gamma=0.01$ and linear amplification of strength $\delta=8.95\times10^{-4}$. Right panel: time evolution of the gap-Townes soliton amplitude in the left panel. Plotted quantities are in normalized units.

Towenes solitons. For the 1D quintic NLS equation with periodic potential the delocalizing transition exists for both attractive and repulsive interactions. Delocalizing curves have been investigated in Figs. 4 and 8. A similar behavior is expected to be valid also for the standard GPE with periodic potential in higher dimensions [39]. The second curve separates the localized solutions from the collapsing ones, giving an upper bound for the existence of gap solitons. This curve obviously exists only for attractive interactions (for repulsive interactions a negative effective mass, although producing an attraction among atoms which leads to the formation of gap solitons, is usually insufficient to induce collapse). Due to the numerical difficulties involved in the study of collapsing solutions, the threshold curves for collapse have not been investigated in this paper. For this it will be useful to develop an analytical approach to provide estimates of the critical values for collapse [40].

We have also investigated the influence of a dissipative imaginary part of the three-body interaction on gap-Townes solitons. In particular, we have shown that the damping introduces effects which are important when the ratio between the imaginary and real parts of the three-body interaction is not small. For the case of rubidium this ratio is expected to be small and the situation described for the underdamped case should be qualitatively valid. We find remarkable, however, that even for moderate large damping a signature of the existence of gap-Townes solitons remains in the focusing-defocusing cycles observed when the number of atoms crosses the critical value for their existence.

Finally, we have shown that the presence of a small linear amplification term in the damped quintic NLS equation, modeling the feeding of atoms from the thermal cloud, can stabilize gap solitons into breatherlike excitations even in presence of large damping.

The results of this paper suggest the possibility to experimentally observe gap-Townes solitons in low-dimensional BEC's.

[1] B. P. Anderson and M. A. Kasevich, Science **282**, 1686 (1998).

[2] M. Cristiani, O. Morsch, J. H. Miller, D. Ciampini, and E. Arimondo, Phys. Rev. A **65**, 063612 (2002).

[3] B. Wu and Q. Niu, New J. Phys. **5**, 104 (2003).

[4] B. Eiermann *et al.*, Phys. Rev. Lett. **91**, 060402 (2003).

[5] M. Greiner, O. Mandel, T. Esslinger, T. W. Hansch, and I. Bloch, Nature (London) **415**, 39 (2002).

[6] B. B. Baizakov, V. V. Konotop, and M. Salerno, J. Phys. B **35**, 5105 (2002).

[7] E. A. Ostrovskaya and Yu. S. Kivshar, Phys. Rev. Lett. **90**, 160407 (2003).

[8] N. Akhmediev *et al.*, Int. J. Mod. Phys. B **13**, 625 (1999).

[9] W. Zhang, E. M. Wright, H. Pu, and P. Meystre, Phys. Rev. A **68**, 023605 (2003).

[10] F. Kh. Abdullaev, A. Gammal, L. Tomio, and T. Frederico, Phys. Rev. A **63**, 043604 (2001).

[11] A. Gammal, T. Frederico, L. Tomio, and F. Kh. Abdullaev, Phys. Lett. A **267**, 305 (2000).

[12] S. Inouye, M. R. Andrews, J. Stenger, H. J. Miesner, D. M. Stampur-Kurn, and W. Ketterle, Nature (London) **392**, 151 (1998).

[13] V. Efimov, Phys. Lett. **33B**, 563 (1970).

[14] A. Bulgac, Phys. Rev. Lett. **89**, 050402 (2002).

[15] P. F. Bedaque, E. Braaten, and H.-W. Hammer, Phys. Rev. Lett. **85**, 908 (2000).

[16] E. Braaten, H.-W. Hammer, and T. Mehan, Phys. Rev. Lett. **88**, 040401 (2002).

[17] Jack W. Michael, Phys. Rev. Lett. **89**, 140402 (2002).

[18] T. Köhler, Phys. Rev. Lett. **89**, 210404 (2002).

[19] E. B. Kolomeisky, T. J. Newman, J. P. Straley, and Qi Xiaoya, Phys. Rev. Lett. **85**, 1146 (2000).

[20] A. Minguzzi, P. Vignolo, M. L. Chiofalo, and M. P. Tosi, Phys. Rev. A **64**, 033605 (2001).

[21] B. Damski, J. Phys. B **37**, L85 (2004).

[22] D. J. Frantzeskakis, N. P. Proukakis, and P. G. Kevrekidis, Phys. Rev. A **70**, 015601 (2004).

[23] M. D. Girardeau and E. M. Wright, Phys. Rev. Lett. **84**, 5239 (2000).

[24] L. Berge, Phys. Rep. **303**, 259 (1998).

[25] V. A. Brazhnyi and V. V. Konotop, Mod. Phys. Lett. B **18**, 627 (2004).

[26] B. V. Gisin, R. Driben, and B. A. Malomed, J. Opt. B: Quantum Semiclassical Opt. **6**, S259 (2004).

[27] C. De Angelis, IEEE J. Quantum Electron. **30**, 818 (1994).

[28] K. D. Moll, A. L. Gaeta, and G. Fibich, Phys. Rev. Lett. **90**, 203902 (2003).

[29] B. A. Malomed, Prog. Opt. **43**, 69 (2001).

[30] Mario Salerno, Laser Phys. **15**, 620 (2005); see also e-print cond-mat/0311630.

[31] Yu. B. Gaididei, J. Schjodt-Eriksen, and P. L. Christiansen, Phys. Rev. E **60**, 4877 (1999).

[32] B. B. Baizakov, B. A. Malomed, and M. Salerno, Europhys. Lett. **63**, 642 (2003).

[33] B. B. Baizakov and M. Salerno, Phys. Rev. A **69**, 013602 (2004).

[34] B. L. Tolra, K. M. O'Hara, J. H. Huckans, W. D. Phillips, S. L. Rolston, and J. V. Porto, Phys. Rev. Lett. **92**, 190401 (2004).

[35] A. Bondeson, M. Lisak, and D. Anderson, Phys. Scr. **20**, 479 (1979); A. Maimistov, Zh. Eksp. Teor. Fiz. **104**, 3620 (1993) [JETP **77**, 727 (1993)].

[36] V. S. Filho, F. Kh. Abdullaev, A. Gammal, and L. Tomio, Phys. Rev. A **63**, 053603 (2001).

[37] G. Fibich, SIAM J. Appl. Math. **61**, 1680 (2001).

[38] Y. Kagan, A. E. Muryshev, and G. V. Shlyapnikov, Phys. Rev. Lett. **81**, 933 (1998).

[39] M. Salerno, B. B. Baizakov, and F. Kh Abdullaev (unpublished).

[40] V. V. Konotop and P. Pacciani (private communication).